RSC Advances

PAPER

View Article Online
View Journal | View Issue

Cite this: *RSC Adv.*, 2017, **7**, 53899

Solvent-free synthesis of the cellulose-based hybrid beads for adsorption of lead ions in aqueous solutions

Y. Li,[ab] M. D. Chen,[b] X. Wan,[c] L. Zhang,[b] X. Wang[a] and H. Xiao*[a]

In this work, the adsorption of Pb^{2+} onto maleic anhydride modified cellulose/diatomite beads (MCDBs) was investigated. Instead of the general process for esterifying the cellulose beads, a solvent free synthesis which needs no catalyst or solvent was used. An appropriate amount of calcium carbonate was added during the formation of MCDBs to increase pore structure after being removed under an acidic condition. The synthesized adsorbent was characterized by FTIR, SEM, and BET. The degree of the carboxyl group of MCDBs was found to be 0.450 mmol g^{-1} based on colloid titration. The effects of pH, temperature, contact time, and the concentration of Pb^{2+} on adsorption were studied in batch mode. The results indicated that the MCDBs had a good adsorption capacity toward Pb^{2+} with the maximum adsorption at 44 mg g^{-1}. The experimental kinetic data fit the pseudo-second order model very well. Moreover, the adsorption process for Pb^{2+} was better described by the Langmuir isotherm model. The regeneration of the MCDBs could be readily accomplished using an HCl (1 M) treatment without lowering the adsorption capacity significantly.

Received 29th August 2017
Accepted 11th November 2017

DOI: 10.1039/c7ra09592a

rsc.li/rsc-advances

1. Introduction

Environmental problems, especially aquatic environments, are a main theme of scientific research now and in recent years. The removal of toxic heavy metal ions from industrial effluents, water supplies, and mine waters has received much attention. Heavy metal ions, such as Cu, Cd, Ni, and Pb, released into the environment affect ecological life, owing to their tendency to accumulate in living organisms, and are highly toxic when absorbed into the body.[1] Heavy metals usually have long residence times. Lead toxicity has been reported to decrease kidney functions and enzymatic activities and cause neuromuscular difficulties.[2] There are also many lead contamination incidents with drinking water reported in some countries.[3] Thus, it is necessary to remove heavy metal ions from wastewater.[4]

Various adsorbent materials have been explored for the removal of heavy metal ions from aqueous solutions. Of all the adsorbent materials, activated carbon has been widely used for the removal of heavy metals at trace levels.[5] However, activated carbon is costly as an absorbent in water treatment. Therefore, the production of low-cost materials, such as cellulose and diatomite, has been a hotspot of research. Cellulose, as one of the natural and green materials, constitutes the most abundant natural polymer resource. However, the adsorption capacity is limited, and the selectivity is low when directly using natural cellulose as an adsorbent. Because there are many hydroxyl groups in the polymer structure,[6] hydrogen bonds form between the molecular chains.[7] Chemical modification, such as esterification, halogenation, oxidation, and etherification, can be used to vary certain properties of cellulose, such as its hydrophilic or hydrophobic character, elasticity, water sorbency, adsorptive or ion exchange capability.[8]

Magali *et al.*[9] synthesized new adsorbents containing carboxyl groups by grafting acrylic acid onto sawdust, which was used for the sorption of Cu^{2+} from aqueous solution. James *et al.*[10] milled aspen wood, then the Milled aspen wood was thermochemically modified with citric acid to improve the copper (Cu^{2+}) ion sorption capacity of the wood. Nada *et al.*[11] modified bagasse fibres using three different chemical methods to remove heavy metal ions from waste water. Very recently, Wang *et al.*[12] reported an eco-friendly sugarcane cellulose-based adsorbent with very high sorption capacities towards Pb^{2+}, Cu^{2+} and Zn^{2+}. The application of such adsorbents was also extended to binary component systems; and the adsorption behaviour was found to be well described by the competitive Langmuir isotherm model. Zhou *et al.*[13] synthesized a low-cost absorbent by a cost-effective chemical modification for dyes and heavy metal ion removal. Yu *et al.*[14] prepared cellulose nanocrystals (CNCs) from cotton, and then the CNCs were chemically modified with succinic anhydride to introduce carboxyl groups

[a]*Department of Chemical Engineering, University of New Brunswick, Fredericton, NB, E3B 5A3, Canada. E-mail: hxiao@unb.ca*

[b]*Jiangsu Key Lab of Atmospheric Environment Monitoring and Pollution Control, School of Environmental Sci & Tech, Nanjing University of Information Science and Technology, Nanjing, China 210044*

[c]*Department of Environmental Science and Engineering, North China Electric Power University, Baoding 071003, China*

on the adsorbents. However, a pyridine reflux was used during the chemical modification, which was not conducive to the development of the environment.

Diatomite, a soft lightweight rock available in large deposits around the world, is a highly porous structure and low-cost material.[15] Attributed to its physical and chemical properties, it has been used as an adsorbent in wastewater treatment.[16] Al-Degs *et al.*[17] improved the intrinsic exchange properties by modification with manganese oxides, and the resulting adsorbent showed a high tendency for adsorbing lead ions from solution. Khraisheh *et al.*[18] modified diatomite by NaOH solution and manganese oxide to improve the adsorption capacity of the diatomite for the removal of heavy metals. However, the powdered diatomite and cellulose might lead to difficulty in the application of the adsorbents. Cellulose-based beads facilitate the easy separation of hybrid adsorbents in batch operation. Yang *et al.*[19] prepared carboxymethyl cellulose hydrogel beads using epichlorohydrin (ECH) as a crosslinking agent and found that the additional carboxyl groups afforded a higher sorption capacity to metal ions as well. Recently, Yu *et al.*[20] successfully prepared porous magnetic cellulose beads *via* a one-pot synthesis, which created a new platform to prepare the cellulose-based functional nanocomposites.

Thus, the aim of the present study was to investigate modified cellulose beads in conjunction with alkali-treated diatomite (MCDBs) as a low-cost material for the removal of Pb ions from aqueous solutions. To enhance the absorption capacity of fibres and to facilitate the recovery of adsorbent, the cellulose fibres were dissolved and regenerated, and then reacted with maleic anhydride. During the formation of adsorbent particles, calcium carbonate was added to further increase the porosity of the adsorbent after being removed under acidic conditions. The effects of solution pH, temperature, initial concentration, and contact time during the adsorption processes were also evaluated.

2. Experimental

2.1 Materials

The cellulose raw material was from filter paper (Qualitative P4, porosity: Medium-Fine; Flow Rate: Slow, Fisher Scientific). Diatomite, hydroxylamine hydrochloride, dithizone, $Pb(NO_3)_2$, $CaCO_3$ powder ($\leq$30 μm), maleic anhydride, and urea were all purchased from Sigma-Aldrich, Canada. NaOH is powder purchased from Fisher Scientific, and, NaOH (0.01 M) and HCl (0.01 M) are solution purchased from Fisher Scientific. Ammonium citrate tribasic and potassium sodium L-tartrate tetrahydrate were obtained from Alfa Aesar. The standard Pb (1.000 g L^{-1}) solution was prepared by dissolving appropriate amounts of Pb $(NO_3)_2$ in distilled water.

2.2 Preparation of cellulose/diatomite beads (CDBs)

The diatomite under a 150 mesh was washed with distilled water to remove fines and other adhered impurities, and then desiccated.[21] Chemical modification was accomplished by treating the diatomite with NaOH (5 mol L^{-1}): 150 g diatomite was mixed with 1 L NaOH, then stirred at 100 °C for 2 h. The resulting samples were washed with distilled water, and desiccated in an oven at 100 °C, then stored in glass bottles.

Cellulose solution (4%) was prepared by dissolving filter paper with NaOH (7 wt%)/urea (12 wt%) at −10 °C; homogenizer (Stanfen, Germany) was used during this process. Then, the treated diatomite and $CaCO_3$ were added at different weight ratios. The mixtures were dropped into HCl (1 mol L^{-1}) using a syringe after being dispersed by the homogenizer. The cellulose/diatomite beads (CDBs) were then washed with distilled water to remove $CaCl_2$ after the reaction between $CaCO_3$ and HCl was accomplished and transferred into acetone immediately. After 24 h, the CDBs were desiccated in a vacuum oven (Fig. 1).[22] The synthesized absorbents were named MCDBs-0, MCDBs-10, MCDBs-20, MCDBs-30, and MCDBs-40 according to the different amount of $CaCO_3$.

2.3 Preparation of maleic anhydride-modified CDBs (MCDBs)

The MCDBs (5 g) were treated with maleic anhydride dissolved in acetone (5 g/40 mL acetone), then the acetone was evaporated at 50 °C in a vacuum oven for 1 h and the residual mixture was heated in an oven at 100 °C for 3 h. The products were washed with distilled water, ethanol, and finally with acetone, and then desiccated in a vacuum oven (Fig. 1).[11] The degree of substitution (DS) of hydroxyl groups in the cellulose due to esterification was determined.

2.4 Degree substitution of hydroxyl groups (charge density)

The surface charge density (degree of substitution of the hydroxyl groups) was determined by colloid titration until zero charge point by a particle charge detector (Mütek PCD-03, Germany). In the test, 0.05 g of MCDBs and 0.01 N poly-DADMAC solution (5 mL) were added in the measuring cell at room temperature with constant stirring for 10 min. Then, titration analysis was conducted for both control and fibre samples by adding the PVSK (0.01 N) into the mixture automatically. The point of zero charge detected by the Mutek titrator corresponded to the amount (*i.e.* volume) of PVSK neutralizing the excessive amount of PDADMAC.[23] The experiment was carried out three times simultaneously. The

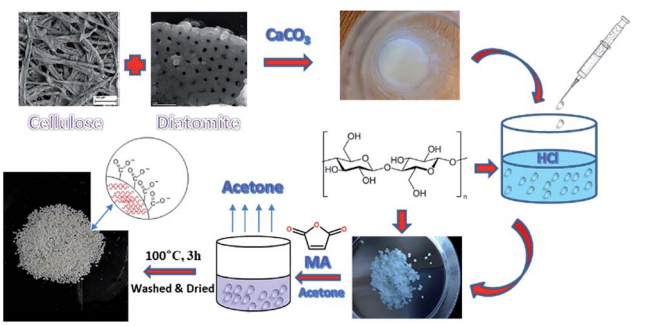

Fig. 1 The solvent-free approach to preparing the cellulose hybrid beads.

concentration of carboxylic functions [C_{COOH} (mmol g^{-1})] was calculated by eqn (1)

$$C_{COOH} = (V_2 - V_1) \times C/m_{MCDBs} \quad (1)$$

where V_2 is the volume of PVSK dropped into the solution with MCDBs (mL), V_1 is the volume of PVSK dropped into the blank solution (mL), C is the concentration of PVSK and poly-Dadmac, and mMCDBs is the mass of the MCDBs (g).

2.5 Characterization

FT-IR spectra were recorded using an NEXUS 470 spectrophotometer (Nicolet Thermo Instruments, Canada) after the MCDBs were ground with KBr. BET adsorption was carried out using an Autosorb instrument (Belsorp-Max BEL Inc, Osaka, Japan). Scanning electron microscopy (SEM) was performed on a JEOL JSM-6400 SEM instrument (Japan).

2.6 Batch experiments

Pb^{2+} was chosen to evaluate the effectiveness of synthesized absorbents for water treatment. All the solutions with various concentrations were obtained by successive dilution. The pH was adjusted by adding either 0.01 M HCl or 0.01 M NaOH. Adsorption experiments were carried out using 10 mL of lead ion solution at the desired concentration (10 mg L^{-1}) at an initial pH of 7.0, and an adsorbent dosage of 0.01 g per 10 mL in an agitation speed of 130 rpm on a temperature-controlled shaker (SWB25, Thermo Electron Corporation, Germany). In the preliminary experiment, this speed was found to be suitable to reach equilibrium. The shaking time, temperature, pH, and the concentration of $CaCO_3$ were investigated, respectively. Residual Pb^{2+} concentration in the filtrate was determined using UV (Genesys 10-s, Thermo Electron Corporation).[24] The percent metal ion removal R (%) was calculated by eqn (2).[25]

$$R = (C_1 - C_e)/C_1 \times 100 \quad (2)$$

where C_1 (mg L^{-1}) and C_e (mg L^{-1}) were the initial and final concentrations of the metal ions, respectively. The adsorption capacity (Q) was calculated by eqn (3).

$$Q = (C_1 - C_e)/m \times V \quad (3)$$

where Q is the adsorption capacity (mg g^{-1}), V is the volume of solution (L) and m is the mass of adsorbent (g) used.

2.6.1 Adsorption kinetics. The pseudo-second-order kinetic model was used to describe the adsorption kinetic data of Pb^{2+} measured on MCDBs. A non-linear form and a linear form are presented in eqn (4) and (5), respectively.[26]

$$dq/dt = k_1(q_e - q)^2 \quad (4)$$

$$t/q_t = 1/(k_1 \times q_e^2) + t/q_e \quad (5)$$

where q_t (mg g^{-1}) and q_e (mg g^{-1}) are the amounts of the Pb^{2+} adsorbed at time t (min) and at equilibrium, respectively. K_1 (g mg^{-1} min^{-1}) is the rate constant of the adsorption process.

2.6.2 Adsorption isotherms. The isotherms were carried out by shaking the MCDBs (0.01 g) with 10 mL of metal ion solution at different initial concentrations. The corresponding adsorption isotherms for lead ions were described by fitting the experimental data to the Langmuir, Freundlich,[27] and Temkin isotherms,[28] respectively. The Langmuir equation used was the linear form eqn (6):[29]

$$C_e/q_e = aC_e/K_L + 1/K_L \quad (6)$$

where q_e and C_e are the solution (mg g^{-1}) and surface concentrations (mg L^{-1}) for the adsorbate at the equilibrium, respectively, and K_L (L g^{-1}) and a (L mg^{-1}) are the isotherm constants. K_L can be obtained from the relationship between C_e/q_e and C_e. The constant, a, corresponds to the energy of the adsorption process. A dimensionless separation factor R_L is the essential characteristic of the Langmuir equation, which is described by eqn (7).[30]

$$R_L = 1/(1 + C_0 \times K_L) \quad (7)$$

where C_0 is the highest initial Pb^{2+} concentration (mg L^{-1}), the value of R_L indicates the nature of the interaction and the isotherm type: unfavourable ($R_L > 1$), linear ($R_L = 1$), favourable ($0 < R_L < 1$), or irreversible ($R_L = 0$).

3. Results and discussion

3.1 FTIR spectra and colloid titration

The FTIR spectra of CDBs before and after modification with maleic anhydride are shown in Fig. 2. The wider peaks at 3442 and 3443 cm^{-1} are due to the stretching of the O–H group. The adsorptions at 2891 and 2897 cm^{-1} are related to the C–H stretching, and the band at 1630 cm^{-1} is attributed to the bending mode of the absorbed water. The absorption bands at 1112 and 1110 cm^{-1} correspond to C–O antisymmetric bridge stretching[31] and siloxane (Si–O–Si) stretching from alkali-treated diatomite.[32] The main difference between CDBs and MCDBs is the new peak at 1724 and 1638 cm^{-1}. The adsorption at 1724 cm^{-1} indicates the carboxyl groups (C=O)[33] and the one at 1638 cm^{-1} relates to vibration of vinyl groups (C=C). The

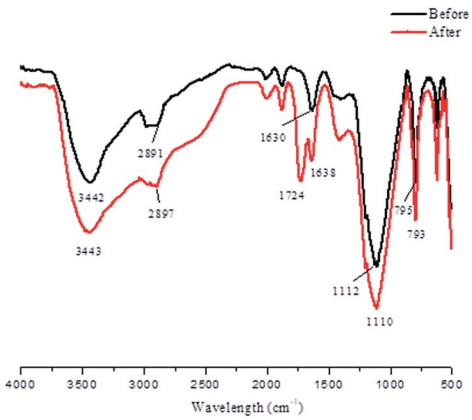

Fig. 2 FTIR spectra of CDBs before and after modification.

–OH stretching adsorption bands at 3442 cm^{-1} do not significantly change after modification. Because only the surface hydroxyls that are available, maleic anhydride can be grafted during the chemical reaction.[34]

According to the results obtained by colloid titration, the concentration of carboxyl groups on the surface of the MCDBs was 0.45 mmol g^{-1}, which corresponds to the surface charge density of MCDBs.

3.2 SEM

The surface structure of cellulose beads obtained was revealed by SEM and the images are shown in Fig. 3. The CDBs obtained exhibited good spherical shape together with a porous structure (Fig. 3(a)). More pores can be observed in Fig. 3(c) and (e) than in Fig. 3(b). The application of $CaCO_3$ was conducive to the pore structure. The pores may be formed from the reaction between $CaCO_3$ and HCl, during which the $CaCO_3$ rich regions were transformed into pores due to the release of carbon dioxide and dissolution of $CaCO_3$. The alkali-treated diatomite exists in CDBs independently (Fig. 3(d)), which can preserve the adsorption capacity of adsorbate. After modification, maleic anhydride was grafted onto cellulose, which leads to decreasing pores in CDBs (Fig. 3(c) and (f)), due to the grafted maleic anhydride which might fill up some pores on the spheres (Fig. 3(g) and (h)). This can be proved with the results of BET.

3.3 Brunauer–Emmett–Teller (BET) adsorption

The specific surface areas of the MCDBs were evaluated by BET analysis; and the results are presented in Table 1. The specific surface area of MCDBs increased significantly when the concentration of $CaCO_3$ changed from 10% to 30%, at the same time, the total pore volume was changed from 5.78×10^{-3} to 9.42×10^{-3} m^3 g^{-1}, which indicates the application of $CaCO_3$ is conducive to the pore structure. After modification with maleic anhydride, the specific surface area of MCDBs reduced to 0.73 m^2 g^{-1}, meanwhile, the total pore volume changed from 9.42×10^{-3} to 4.89×10^{-3} m^3 g^{-1}, implying the grafted maleic anhydride might fill up some pores. However, the adsorption capacity of MCDBs (30% $CaCO_3$) is much lower than that MCDBs-30 (after modification), which means the esterification is the main reason for the increase in the adsorption capacity of Pb^{2+} onto MCDBs. MCDBs-40 does not have any results from BET, which might be due to the collapse of the pores. In addition, the specific surface area of MCDBs-0 could not be detected by BET, which indicate that MCDBs-0 had very limited or no micro or mesoporous structures.

Table 1 The BET results of CDBs and MCDBs

MCDBs	Specific surface(m^2 g^{-1})	Pore volume(m^3 g^{-1})
MCDBs-0 (before modification)	—	$1.1x10^{-3}$
MCDBs-10 (before modification)	1.00	$5.78x10^{-3}$
MCDBs-20 (before modification)	1.21	$6.64x10^{-3}$
MCDBs-30 (before modification)	1.53	$9.42x10^{-3}$
MCDBs-30 (after modification)	0.73	$4.89x10^{-3}$
MCDBs-40 (before modification)	—	$6.23x10^{-3}$

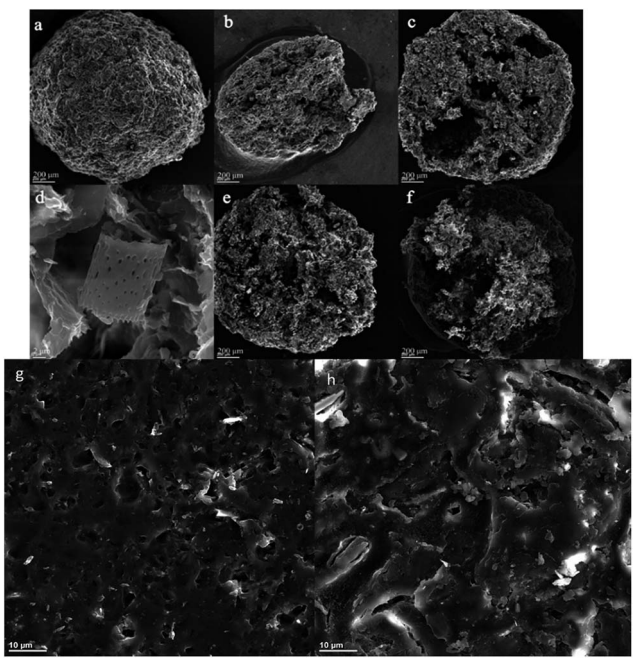

Fig. 3 SEM images of surface morphology (a), cross-section structure of MCDBs-10 (10% $CaCO_3$) (b), MCDBs-30 (30% $CaCO_3$) before modification (c, d, and g), MCDBs-30 (30% $CaCO_3$) after modification (f, h), MCDBs-40 (40% $CaCO_3$) (e) of regenerated cellulose beads.

3.4 Comparative test

The Pb^{2+} removal rate (%) of different absorbents, including raw materials, CDBs and MCDBs, are shown in Fig. 4. The adsorption capacity of raw materials is extremely low, which is 44.95% for filter paper and 9.30% for alkali-treated diatomite, respectively. The CDBs have a higher removal rate compared with the raw materials. Furthermore, the adsorption capacity of Pb^{2+} significantly increased after the modification by maleic anhydride. These results demonstrated that the MCDBs are good carriers or adsorbents toward Pb^{2+}. The effect of $CaCO_3$ concentration was studied at room temperature and neutral pH, and the results are also shown in Fig. 4. The removal rate (%) increased significantly with the initial concentration of $CaCO_3$ increase from 0% to 30%, and the removal rate was negatively affected when further increasing the concentration of $CaCO_3$ up to 40%, because the $CaCO_3$ at an over-dosage can induce the collapse of CDB pores. Therefore, $CaCO_3$ play a role in the pore structure; the optimum concentration of $CaCO_3$ is 30%.

3.5 Effect of pH

The removal of Pb^{2+} from aqueous solutions by adsorption depends on the pH, which affects the ionization of metal ions and the concentration of counter H^+ ions on the surface of the adsorbent. To study the effect of H^+ concentration on metal

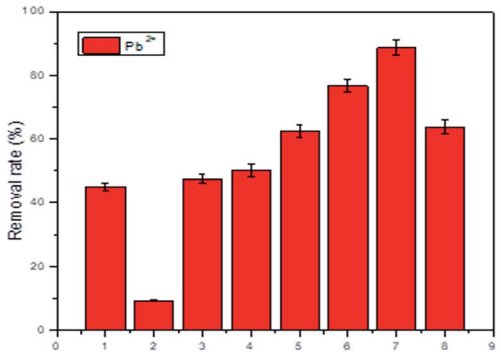

Fig. 4 Removal rate of different materials: (1) filter paper; (2) alkali-treated diatomite; (3) CDBs-0; (4) MCDBs-0; (5) MCDBs-10; (6) MCDBs-20; (7) MCDBs-30; (8) MCDBs-40.

removal, the solution pH was varied from 2 to 6. The results are shown in Fig. 5.

The optimum pH value for the adsorption of Pb^{2+} by MCDBs was found to be pH 6.0 (Fig. 5). For MCDBs-30, the percentage removal rate is observed to be 88.89% for Pb^{2+} adsorption at this pH. In aqueous solutions, Pb^{2+} is dominant at pH 2–6. Other species ($PbOH^{+}$) can exist at a higher pH. The removal rate of Pb^{2+} is extremely low at a pH below 3. The higher the concentration of H_3O^{+}, which means a lower pH, the higher the concentration of protons competing with metal ions for the active sites. The surface of absorbents is positively charged, and it is hard to adsorb heavy metals with a positive charge.[35,36] With increasing pH (pH > 3), the concentration of protons decreased, and the surface is negatively charged, which is advantageous for adsorption.

3.6 Effect of temperature

The effects of temperature on the adsorption of Pb^{2+} were studied by changing the temperature from 15 to 50 °C under the optimum pH in 2 h; the results are presented in Fig. 6. The adsorption of Pb^{2+} increased significantly as the temperature changed from 20 to 30 °C, which indicates that the adsorption process on MCDBs is an endothermic process. It changes indistinctively after 30 °C. So, the optimum temperature of Pb^{2+} adsorption on MCDBs is selected to be 30 °C.

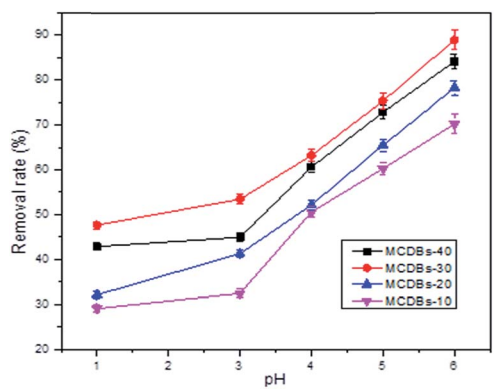

Fig. 5 Effect of pH on the adsorption of Pb^{2+}.

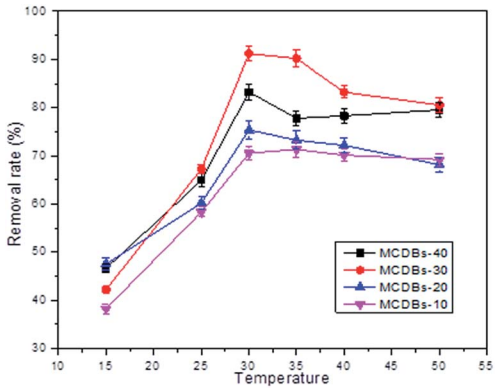

Fig. 6 Effect of temperature on the adsorption of Pb^{2+}.

3.7 Adsorption behaviour

3.7.1 Adsorption kinetics. The effect of contact time on the adsorption of Pb^{2+} by MCDBs-30 is shown in Fig. 7 and the results of adsorption kinetics, calculated from Fig. 7, are shown in Fig. 8. Experiments were performed at different temperatures (20, 30 and 45 °C) at pH 6. During short contact times, the adsorption process is very fast (within 10 min more than 50% is adsorbed) due to the numerous active sites on the surface of MCDBs-30; then, the removal rate levelled off. Over 84% adsorption efficiency is obtained at a certain temperature, indicating that Pb^{2+} is absorbed by available adsorption sites. The sorption of Pb^{2+} onto MCDBs-30 is mainly mediated through complexation with surface functional groups (especially carboxyl groups) which can react with Pb^{2+} to form bound complexes.[37]

The adsorption process for Pb^{2+} is described by a pseudo-second-order model, where R^2 is 0.9959, 0.9950, and 0.9981 at the temperatures of 20, 30 and 45 °C, respectively (Fig. 8). The fitting results suggested that the adsorption rate was dominated by chemical adsorption, which involved the electron sharing or electron transfer between the adsorbent and the adsorbate. The q_e values for Pb^{2+} adsorption are in good agreement with the experimental one. This indicates a good agreement that the pseudo-second-order model describes the kinetics of the adsorption.[38]

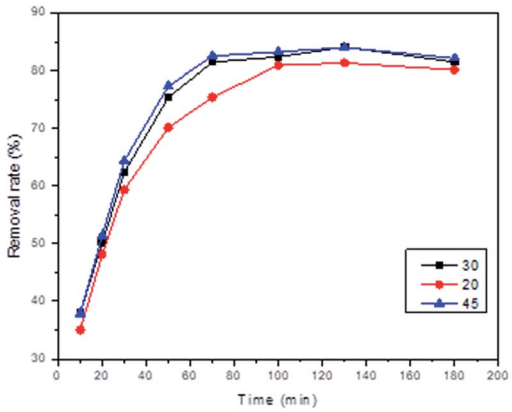

Fig. 7 Effect of contact time on the adsorption of Pb^{2+}.

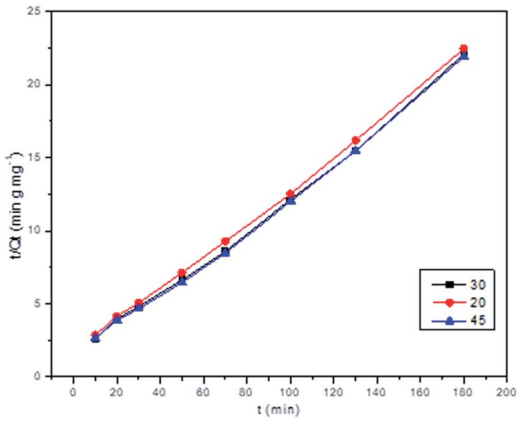

Fig. 8 Pseudo-second-order adsorption kinetics on MCDBs.

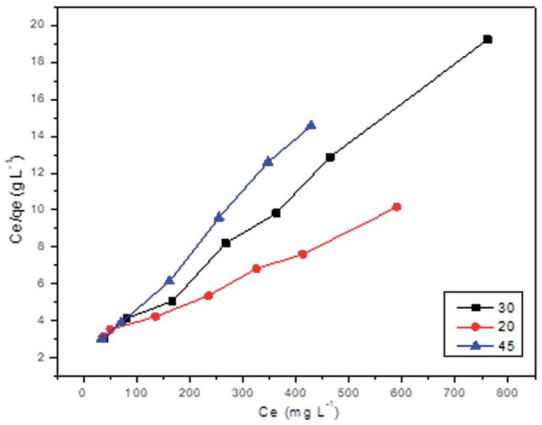

Fig. 9 Linear plots of the Langmuir isotherm for the adsorption on MCDBs.

3.7.2 Adsorption isotherms. The results of adsorption isotherms, calculated from different models, are shown in Table 2 and Fig. 9. A Langmuir model fits the experimental data well and the correlation coefficients of the equations (R^2 = 0.9952) indicate that this model can explain the adsorption process satisfactorily. The Langmuir isotherm is monolayer sorption where the adsorption sites are the same and the absorbed particles are independent, and therefore no further sorption can take place after a saturation value is reached.[39] In this study, the R_L value is between 0 and 1, which indicates that the adsorption process is favourable. The estimated q_m = 46.04 mg g^{-1} (K_L/a) is very close to the experimentally (44.54 mg g^{-1}) obtained maximum metal uptake for Pb^{2+}. Monolayer adsorption capacities for the adsorption of Pb^{2+} onto MCDBs-30 and other materials are compared in Table 3.

In addition, the thermodynamic parameters, such as enthalpy (ΔH°), entropy (ΔS°) and Gibb's free energy (ΔG°), were estimated using the Van't Hoff equation. Table 4 lists the thermodynamic parameters obtained from the temperature effect on Pb^{2+} adsorption, and the values of free energy changes ΔG° are negative, confirming that the adsorption of Pb^{2+} onto MCDBs is spontaneous and thermo-dynamically favourable. The ΔG° value decreased as the temperature increased, indicating a lower driving force for the adsorption. The negative values of ΔH° and ΔS° indicate that the Pb^{2+} adsorption on MCDBs was exothermic in nature and the stability of the adsorption process, with no structural change at solid–liquid interface.

3.8 Desorption of Pb^{2+} from MCDBs-30

Desorption of the Pb^{2+} was investigated. This procedure is necessary to restore the original adsorption capacity of the adsorbent and it also enables recovering valuable metals from wastewater streams. In this study, Pb^{2+} was desorbed from MCDBs-30 using 1 M HCl for 24 h. Then the absorbent was washed with distilled water, ethanol, and finally acetone. The absorbent was reused three times at the same conditions (Pb^{2+} concentration: 10 mg L^{-1}; adsorbent: 0.01 g; volume of solution: 0.01 L), resulting in the removal rates (%) at 94.96, 90.74, and 87.13, respectively. The removal rate of Pb^{2+} is substantially unchanged after reusing three times (the third time is 87.13%), indicating that the MCDBs-30 are a renewable absorbent for Pb^{2+} removal.

Table 3 Results for the adsorption of Pb^{2+} by MCDBs and other materials

Absorbent materials	Adsorbent capacity (mg g^{-1})
Pine cones[40]	27.53
Soybean hulls[41]	44.37
MCDBs-30	44.54
Kaolinite clay[42]	113.63
Apricot stone[43]	22.85

Table 2 The isotherm models for Pb^{2+} adsorption

Adsorbate	Isotherm models	K_L	a	K_f	n	A	b_T	R^2
Pb^{2+}	Langmuir (20 °C)	0.3776	0.0047	—	—	—	—	0.9949
	Langmuir (30 °C)	0.5109	0.0116	—	—	—	—	0.9952
	Langmuir (45 °C)	0.5666	0.0171	—	—	—	—	0.9958
	Freundlich (20 °C)	—	—	3.552	1.649	—	—	0.9732
	Freundlich (30 °C)	—	—	3.606	2.601	—	—	0.8921
	Freundlich (45 °C)	—	—	3.596	2.784	—	—	0.9141
	Temkin (20 °C)	—	—	—	—	0.3095	29.07	0.9268
	Temkin (30 °C)	—	—	—	—	0.3607	53.91	0.9706
	Temkin (45 °C)	—	—	—	—	0.4064	80.02	0.8711

Table 4 The calculation of ΔG°, ΔH°, and ΔS°

Temperature (K)	ΔG° (kJ mol^{-1})	ΔS° (kJ mol^{-1} K^{-1})	ΔH° (kJ mol^{-1})
293.15	−1.285	−0.0604	−20.66
298.15	−1.137		
303.15	−1.045		
318.15	−0.623		

4. Conclusion

Maleic anhydride modified CDBs (combine cellulose and alkali-treated diatomite) was found to effectively adsorb Pb^{2+} from aqueous solutions. The pore structure of the absorbents was enhanced by introducing $CaCO_3$ during the preparation. Further experiment data revealed that the adsorption process of Pb^{2+} on the MCDBs-30 follows a pseudo-second-order kinetics and the equilibrium data can be well fitted with a Langmuir isotherm. The maximum adsorption capacities of adsorbent (Langmuir) was 44 mg g^{-1} from an initial concentration of 800 mg L^{-1} at pH 6 and at 30 °C. The capacity of the adsorbents in Pb^{2+} removal remained unchanged after reusing three times. The MCDBs-30 is a green-based, cost-effective, and renewable absorbent. It could be used to adsorb more heavy metal ions which are positive charged.

Conflicts of interest

There are no conflicts to declare.

Acknowledgements

Financial support for this work from NSERC Canada, NSF China (No. 51379077), NSF China (No. 21272118) and Jiangsu provincial NSF (BK20131429) is gratefully acknowledged.

Notes and references

1 B. Volesky and Z. R. Holan, *Biotechnol. Prog.*, 1995, **11**, 235–250.
2 H. G. Seiler, H. Sigel and A. Sigel, *Handbook on toxicity of inorganic compounds*, Marcel Dekker, New York, 1988.
3 K. Li and X. Wang, *Bioresour. Technol.*, 2009, **100**, 2810–2815.
4 J. Mohsen and A. Fathemeh, *J. Mater. Cycles Waste Manage.*, 2013, **15**, 548–555.
5 K. S. Low, C. K. Lee and S. M. Mak, *Wood Sci. Technol.*, 2004, **38**, 629–640.
6 X. F. Ma, C. Z. Liu, D. P. Anderson and P. R. Chang, *Chemosphere*, 2016, **165**, 399–408.
7 C. Emo, C. Andrea, D. Selvatore and S. Roberto, *Prog. Polym. Sci.*, 2003, **28**, 963–1014.
8 D. J. McDowall, B. S. Gupta and V. T. Stannett, *Prog. Polym. Sci.*, 1984, **10**, 1–50.
9 G. Magali, M. Veronique, C. Andre, L. Bernard and G. Philippe, *J. Wood Sci.*, 2000, **46**, 331–333.
10 D. M. James, M. R. Roger and M. S. Hong, *J. Nat. Fibers*, 2006, **3**, 43–58.
11 A. M. A. Nada and M. L. Hassan, *J. Appl. Polym. Sci.*, 2006, **102**, 1399–1404.
12 F. T. Wang, Y. F. Pan, P. X. Cai, T. X. Guo and H. N. Xiao, *Bioresour. Technol.*, 2017, **241**, 482–490.
13 Y. Zhou, Q. Jin, X. Hu, Q. Zhang and T. Ma, *J. Mater. Sci.*, 2012, **47**, 5019–5029.
14 X. Yu, S. Tong, M. Ge, L. Wu, J. Zuo, C. Cao and W. Song, *J. Environ. Sci.*, 2013, **25**, 933–943.
15 M. A. M. Khraisheh, Y. S. Al-degs and W. A. M. Mcminn, *Chem. Eng. J.*, 2004, **99**, 177–184.
16 P. Pusit, T. Pilaiporn and P. Sukon, *J. Microsc.*, 2011, **4**, 103–107.
17 Y. Al-Degs, M. A. M. Khraisheh and M. F. Tutunji, *Water Res.*, 2001, **35**, 3724–3728.
18 M. A. M. Khraisheh, M. A. Al-Ghouti, S. J. Allen and M. N. M. Ahmad, *Water Environ. Res.*, 2004, **76**, 2655–2663.
19 S. P. Yang, S. Y. Fu, H. Liu, Y. M. Zhou and X. Y. Li, *J. Appl. Polym. Sci.*, 2011, **119**, 1204–1210.
20 X. Yu, D. Kang, Y. Hu, S. Tong, M. Ge, C. Cao and W. Song, *RSC Adv.*, 2014, **4**, 31362–31369.
21 W. S. Moore, D. Reid and J. Geophys, *J. Geophys. Res.*, 1973, **78**, 8880–8886.
22 Y. Li, H. Xiao, M. Chen, Z. Song and Y. Zhao, *J. Mater. Sci.*, 2014, **49**, 6696–6704.
23 A. Musyanovych, R. Rossmanith, C. Tontsch and K. Landfester, *Langmuir*, 2007, **23**, 5367–5376.
24 Y. Wang and M. Zhu, *Sci. Technol. Food Ind.*, 2006, **8**, 164–165.
25 K. Mukhopadhyay, A. Ghosh, S. K. Das, B. Show, P. Sasikumar and U. C. Ghosh, *RSC Adv.*, 2017, **7**, 26037–26051.
26 Y. He, T. Xu, J. Hu, C. Peng, Q. Yang, H. Wang and H. Liu, *RSC Adv.*, 2017, **7**, 30500–30505.
27 X. Jiang, S. Wang, L. Ge, F. Lin, Q. Lu, T. Wang, B. Huang and B. Lu, *RSC Adv.*, 2017, **7**, 38965–38972.
28 Z. Chen, W. Ma and M. Han, *J. Hazard. Mater.*, 2008, **155**, 327–333.
29 F. Lu, C. Huang, L. You, J. Wang and Q. Zhang, *RSC Adv.*, 2017, **7**, 23255–23264.
30 G. McKay, *J. Chem. Technol. Biotechnol.*, 1982, **32**, 759–772.
31 Q. Lu, X. Li, L. Tang, B. Lu and B. Huang, *RSC Adv.*, 2015, **5**, 56198–56204.
32 Y. Al-Degs, M. A. Khraisheh and M. F. Tutunji, *Water Res.*, 2001, **35**, 3724–3728.
33 H. Sanna, R. Evelliina and S. Mika, *Chem. Eng. J.*, 2013, **223**, 40–47.
34 H. Zhao, J. H. Kwak, Z. C. Zhang, H. M. Brown, B. W. Arey and J. E. Holladay, *Carbohydr. Polym.*, 2007, **68**, 235–241.
35 Z. X. Wang, G. Li, F. Yang, Y. L. Chen and P. Gao, *Carbohydr. Polym.*, 2011, **86**, 1807–1813.
36 M. Iqbal, A. Saeed and I. Kalim, *Sep. Sci. Technol.*, 2009, **44**, 3770–3791.
37 J. H. Park, Y. S. Ok, S. H. Kim, J. S. Cho, J. S. Heo, R. D. Delaune and D. C. Seo, *Chemosphere*, 2016, **142**, 77–83.

38 M. D. Ahmed, A. A. Asem and S. Y. Shereen, *J. Dispersion Sci. Technol.*, 2013, **34**, 1230–1239.
39 Z. H. Ding, R. Yu, X. Hu, Y. J. Chen and Y. F. Zhang, *Cellulose*, 2014, **21**, 1459–1469.
40 M. Milan, M. Milovan, B. Aleksandar, Z. Aleksandra and R. Marjan, *Desalination*, 2011, **276**, 53–59.
41 M. M. Johns, W. E. Marshall and C. A. Toles, *J. Chem. Technol. Biotechnol.*, 1998, **71**, 131–140.
42 O. Waid and A. Hossam, *Am. J. Appl. Sci.*, 2007, **4**, 502–507.
43 M. Kobya, E. Demirbas, E. Senturk and M. Ince, *Bioresour. Technol.*, 2005, **96**, 1518–1521.